Heat capacity and magnetic properties of fluoride $CsFe^{2+}Fe^{3+}F_6$ with defect pyrochlore structure

M.V. Gorev [a,b,*], I.N. Flerov [a,b], A. Tressaud [c], E.V. Bogdanov [a,d], A.V. Kartashev [a,e], O.A. Bayukov [a], E.V. Eremin [a,b], A.S. Krylov [a]

[a] *Kirensky Institute of Physics, Russian Academy of Sciences, Siberian Branch, 660036 Krasnoyarsk, Russia*
[b] *Institute of Engineering Physics and Radio Electronics, Siberian State University, 660074 Krasnoyarsk, Russia*
[c] *Institut de Chimie de la Matière Condensée, ICMCB-CNRS, Université Bordeaux, 33608 Pessac Cedex, France*
[d] *Astafijev Krasnoyarsk State Pedagogical University, 660049 Krasnoyarsk, Russia*
[e] *Krasnoyarsk State Agrarian University, 660049 Krasnoyarsk, Russia*

ARTICLE INFO

ABSTRACT

Heat capacity, Mössbauer and Raman spectra as well as magnetic properties of fluoride $CsFe_2F_6$ with defect pyrochlore structure were studied. In addition to recently found above room temperature three successive structural transformations Pnma-Imma-I4$_1$amd-Fd-3m, phase transition of antiferromagnetic nature with the 13.7 K Neel temperature and a broad heat capacity anomaly with a maximum at about 30 K were observed. The room temperature symmetry Pnma is unchanged at least down to 7 K. Simple model of indirect bond used to estimate the exchange interactions and to propose a magnetic structure model.

© 2016 Elsevier Inc. All rights reserved.

1. Introduction

A lot of fluoride, oxide, as well as oxyfluoride compounds crystallize in cubic or distorted pyrochlore structures. Fluorides with $AMe^{2+}Me^{3+}F_6$ general chemical formula exhibit at ambient conditions various symmetries (P2$_1$/c, Imma, Pnma, Fd-3m) depending on the relation between the size of divalent and trivalent metal atoms [1]. For example a series of crystals $AMe^{2+}Fe^{3+}F_6$ with fixed trivalent iron atom exhibits at room temperature either Fd-3m (Me^{2+}: Mn, Co, Zn, Mg, Ni), or Pnma (Me^{2+}: Fe, Ag) symmetry [1]. Because of the important chemical pressure associated with change of the unit cell volume occurring for cationic/anionic substitution, a high probability of symmetry change with temperature in fluoride pyrochlores can be anticipated. However, for fluorides and oxyfluorides with the cubic pyrochlore structure (sp. gr. Fd-3m) at ambient conditions, there is no example, contrary to oxides, of the occurrence at lower temperature of a phase exhibiting a lower symmetry. On the other hand, the transformation of a room temperature orthorhombic phase into a cubic one was recently observed on heating $CsFe^{2+}Fe^{3+}F_6$ [2]. The process was found to consist of three first-order successive structural phase

transitions Pnma (Z=4)↔Imma (Z=4)↔I4$_1$/amd (Z=4)↔Fd-3m (Z=8), occurring within a rather narrow temperature range, i.e. between 500 K and 560 K. In the cubic pyrochlore structure (Z=8, Fd-3m) the cations Fe^{2+}/ Fe^{3+} are disordered in the (16c) position. All distorted phases are cation-ordered. In Pnma phase Fe^{2+} and Fe^{3+} ions form distinct sublattices consisting of chains which run parallel to [100] and [010] of the orthorhombic cell.

Taking into account that many other crystal families having Pnma symmetry at high temperature undergo on cooling structural phase transitions accompanied with the symmetry lowering [3], one could be supposed that a similar situation could be observed in fluorides with the same initial orthorhombic symmetry. Neutron diffraction studies of $NH_4Fe^{2+}Fe^{3+}F_6$ and $RbFe^{2+}Fe^{3+}F_6$ did not show any change from the Pnma space group down to ~4 K [4,5]. Experiments with differential scanning calorimeter on $CsFe^{2+}Fe^{3+}F_6$ also did not show any transformations at least down to 100 K [2]. However, it can be noted that symmetry decrease of the room temperature orthorhombic phase in $CsFe^{2+}Fe^{3+}F_6$ on cooling is not forbidden in accordance with a group-to-subgroup relation between space groups Pnma and for example P2$_1$/c, as observed in some related fluoride compounds [1]. At the same time, $AMe^{2+}Fe^{3+}F_6$ compounds as well as many others of $AMe^{2+}Me^{3+}F_6$ and $AMe^{2+}(Me')^{3+}F_6$ series show peculiar magnetic properties associated, as a rule, with the antiferromagnetic ordering at rather low temperatures [4–8]. In addition to the aforementioned magnetic behavior, magnetic

* Corresponding author at: Kirensky Institute of Physics, Russian Academy of Sciences, Siberian Branch, 660036 Krasnoyarsk, Russia.
E-mail address: gorev@iph.krasn.ru (M.V. Gorev).

frustration has been pointed out [4,5].

In the present paper, we investigate the physical properties of $CsFe^{2+}Fe^{3+}F_6$ through heat capacity, Raman and Mössbauer spectroscopies and magnetization at and below room temperature. This material represents an example of a charge-ordered pyrochlore-related mixed-metal fluoride that exhibits strong magnetic frustration. In addition to the magnetic, thermal and spectroscopic measurements, some theoretical calculations are performed.

2. Results and discussion

2.1. Preparation and characterization

Experiments were carried out on the $CsFe^{2+}Fe^{3+}F_6$ sample examined earlier by us above room temperature using differential scanning calorimetry (DSC) and X-ray powder diffractometry [2]. Pyrochlore under study was prepared by solid state synthesis of the binary fluorides, CsF, FeF_2 and FeF_3, in sealed platinum tube. Iron fluorides, FeF_2 and FeF_3, were obtained by fluorination of $FeCl_2$ and $FeCl_3$ under a stream of anhydrous HF at 400 °C and in pure F_2 atmosphere at 300 °C, respectively, for several hours. Thoroughly dehydration of CsF was performed before use.

The detailed structural characterization of the obtained $CsFe_2F_6$ was performed in Ref. [2]. The room temperature symmetry is orthorhombic Pnma. No additional phases were found.

In order to clarify the distribution of Fe ions on the different crystallographic sites, Mössbauer spectra were recorded on a MC-1104Em spectrometer with a Co^{57} (Cr) source at room temperature on powder samples. Spectra represent the sum of quadrupole doublets with different intensity and splitting (Fig. 1(a)).

Identification of spectra was performed in two stages. In a first step probability distribution of the quadrupole splitting in experimental spectra was defined. The sum of two groups of quadrupole doublets with a natural width was used. Amplitudes of doublets and two isomer chemical shifts corresponding to two groups of doublets were obtained by fitting (Fig. 1(a)). Probability distribution of quadrupole splitting for two valences states of iron, Fe^{3+} and Fe^{2+}, is shown in Fig. 1(b). Distribution $P(QS)$ for $CsFe_2F_6$ shows two narrow single maxima. It means that Fe^{3+} and Fe^{2+} cations are ordered in the lattice positions of the pyrochlore structure.

In the second step the model spectrum was formed on the basis of information about the nonequivalent positions of Fe^{3+} and Fe^{2+} ions resulting from $P(QS)$. The model spectrum was fitted to the experimental one by varying all hyperfine parameters. The results of fitting are presented in Table 1.

Values of chemical shifts, (Table 1), correspond to high-spin for both cations, Fe^{3+} and Fe^{2+}, occupying octahedral positions. Occupations of Fe^{3+} and Fe^{2+} differ a little bit probably because of an experimental error and difference of Mössbauer effect for these cations.

The ordered distribution of Fe^{3+} and Fe^{2+} ions in crystal lattice and obtained values of isomer chemical shift, quadrupole splitting and width of Mössbauer lines agree with the results obtained earlier for $CsFe_2F_6$ and related compounds [2,9,10].

The non-equivalency of the sub-spectrum areas for Fe^{3+} and Fe^{2+} ions (Table 1) is consistent with the following refined chemical formulation $Cs_{0.94}Fe^{2+}_{0.94}Fe^{3+}_{1.06}F_6$. However, taking into account the uncertainty of A value, one can say that we deal with a compound close to theoretical pyrochlore formula, $CsFe^{2+}Fe^{3+}F_6$.

2.2. Heat capacity and Raman spectra

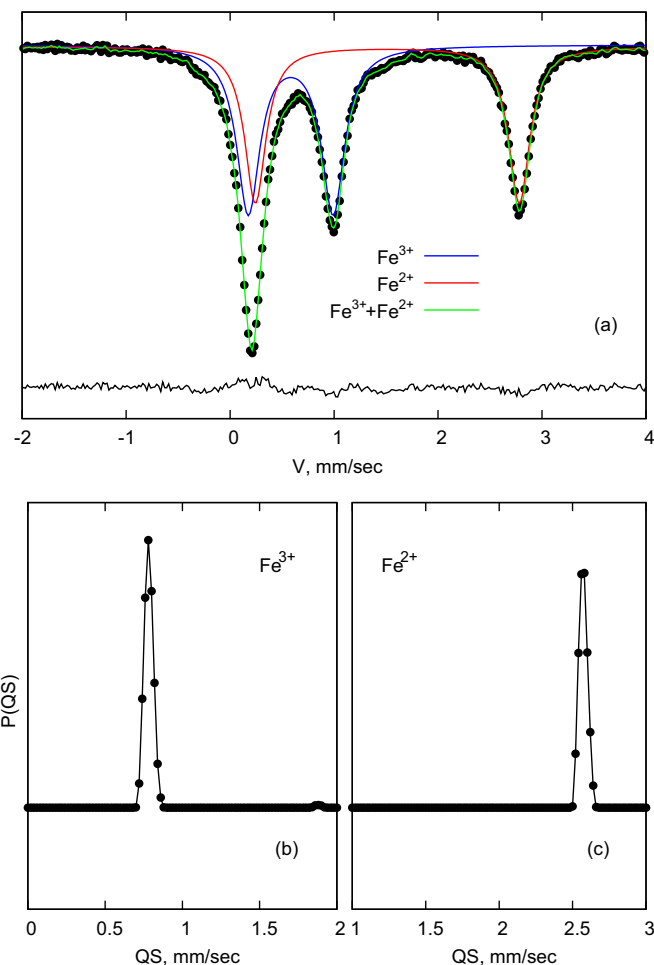Recently, we have performed preliminary DSC investigations on

Fig. 1. Mössbauer spectra of $CsFe_2F_6$ (a). Probability distribution of quadrupole splittings in experimental spectra for Fe^{3+} (b) and Fe^{2+} (c) cations.

Table 1
Mössbauer parameters of $CsFe_2F_6$. IS – isomer chemical shift relative to α-Fe, QS – quadrupole splitting, W – linewidth, A – area of sub-spectrum (occupancy of individual position).

IS, mm/s ± 0.005	QS, mm/s ± 0.01	W, mm/s ± 0.01	A ± 0.003	Position
0.429	0.82	0.27	0.53	Fe^{3+}
1.358	2.54	0.25	0.47	Fe^{2+}

the anomalies of heat capacity in $CsFe_2F_6$ between 100 and 700 K [2]. The succession of three structural phase transitions was found in the 500–560 K temperature range. On the other hand, no anomalous behavior of heat capacity was observed below room temperature. Taking into account the rather low sensitivity of DSC method toward small heat effects associated for example with the second order phase transitions of displacive type, detailed calorimetric studies on $CsFe_2F_6$ were carried out in the present paper using a special option of a Physical Property Measurement System (PPMS, Quantum Design, USA). Measurements were performed on a ceramic sample with a mass of about 35.24 mg in the temperature range 4–300 K. Apiezon N grease was used to provide reliable thermal contact between the sample and the additives. The absolute accuracy of measurements was better than 1%.

Data on the molar isobaric heat capacity, $C_p(T)$, as a function of temperature are plotted in Fig. 2(a). In the temperature range studied only one distinct anomaly of a heat capacity was observed with the maximum value at about 13.7 ± 0.3 K.

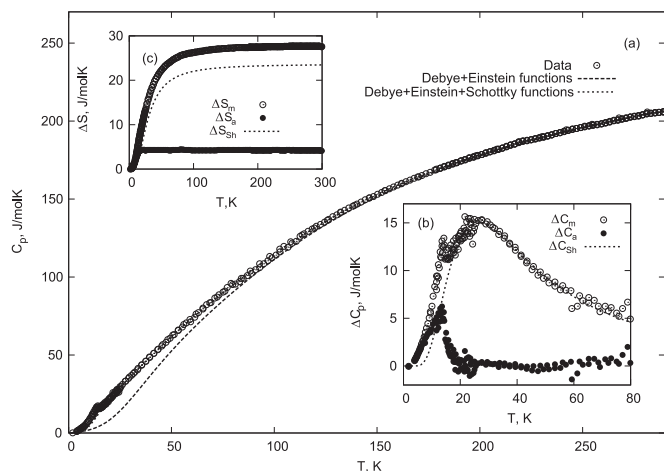To be sure that heat capacity anomaly is not associated with the

Fig. 2. Temperature dependencies of heat capacity (a), magnetic heat capacity contributions (b), and magnetic entropy (c) for CsFe$_2$F$_6$.

Table 2
Normal Raman active modes of the octahedron vibrations.

Type of vibration	Wavenumber, cm^{-1} [12,13]	Wavenumber, cm^{-1} [This work]
F$_{2g}$	253	319
E$_g$	374	
	467	
A$_{1g}$	538	550

change of crystal structure, Raman spectra were analyzed at room temperature and 7 K. Spectrometer Horiba Jobin Yvon T64000 with Ar$^+$-laser ($\lambda=514.5$ nm) was used. Temperature measurements were carried out with a closed cycle helium cryostat ARS CS204-X1.SS at pressure $p=10^{-6}$ mbar. The sample was placed in indium packing and fixed on the cold conductor of cryostat.

The results of measurements are shown in Fig. 3. The presence of an additional contribution to the background of intensities at low temperature is due to the effect of the In contact. As seen in Fig. 3, there are no any splitting nor significant shift of the main peaks in low temperature spectrum associated with the frequency vibrations of the atoms compared to room temperature one. This clearly demonstrates that the symmetry of CsFe^{2+}Fe^{3+}F$_6$ remains orthorhombic at least down to 7 K. The peaks with a frequency lower than 600 cm^{-1} correspond mainly to the vibrations of the FeF$_6$ octahedra. Table 2 shows the relation between the normal modes, as well as characteristic frequencies of the octahedron vibrations in CsFe$_2$F$_6$ and some other hexafluorometallates [11–13].

To extract the associated magnetic heat capacity contribution ΔC_m in the absence of a suitable non-magnetic analog of compound studied, the lattice part C_L is estimated often by fitting the data with an equation consisting of the linear combination of Debye and Einstein terms $C_L=K_D C_D+ K_E C_E$. Unfortunately, in low temperature region such a description of C_L is not relevant and it is not possible to get a correct extraction of magnetic heat capacity components connected with magnetic phase transition ΔC_a and/ or with potential splitting of magnetic levels of Fe ions in crystal

field (Schottky anomaly) C_{Sh}. For a more accurate determination of the magnetic contributions to heat capacity $\Delta C_m=C_{Sh}+\Delta C_a$, results of ab initio calculations or experimental data from phonon spectra are necessary.

Nevertheless, we tried to describe heat capacity at $T \geq 30$ K, i.e. far from phase transition temperature, by linear combination of Debye and Einstein functions with additional Schottky term $K_D C_D$ $(T)+ K_E C_E(T)+ C_{Sh}(T, K_1, K_2)$ where

$$C_D = 9R\left(\frac{T}{\Theta_D}\right)^3 \int_0^{\Theta_D/T} \frac{x^4 \exp(x)}{(\exp(x) - 1)^2}dx,$$

$$C_E = 3R\left(\frac{\Theta_E}{T}\right)^2 \frac{\exp(\Theta_E/T)}{\left(\exp(\Theta_E/T) - 1\right)^2},$$

$$C_{Sh} = K_1\left(\frac{K_2}{T}\right)^2 \frac{\exp(K_2/T)}{\left(1 + \exp(K_2/T)\right)^2}$$

and $K_D, K_E, K_1, K_2, \Theta_E, \Theta_D$ are fitting parameters.

The results are shown in Fig. 2(a) and (b). The anomalous part ΔC_m was found in a rather wide temperature range 2–150 K and exhibits, apart from the sharp peak at 13.7 K, a broad anomaly with a maximum at about 30 K. The appearance of a broad maximum of ΔC_m has also been noticed for many magnetically frustrated pyrochlore materials which exhibit spin-glass-like behavior, such as NH$_4$CoAlF$_6$, R$_2$Mo$_2$O$_7$ (R=Y, Sm, Gd), R$_2$Mn$_2$O$_7$ (R=Y, Ho, Yb), PbCuTe$_2$O$_6$ and others [8,14,15].

Now, we can estimate the magnetic ΔS_m, anomalous (connected with phase transition) ΔS_a and Schottky ΔS_{sh} entropies presented in Fig. 2(c). It can be seen that $\Delta S_m=\Delta S_{Sh}+\Delta S_a=23.3$ J/ molK+4.4 J/molK=28.7 J/molK is close to maximum magnetic entropy $\Delta S_m=R\ln(6)+R\ln(5)=28.3$ J/molK for Fe^{2+} and Fe^{3+} ions which are in high-spin states (Fe^{3+}: $I=5/2$, Fe^{2+}: $I=2$) according to Mössbauer data.

2.3. Magnetic properties

As for the heat capacity, the magnetic properties of the CsFe$_2$F$_6$ ceramic samples prepared in the form of cylinder (4 mm in diameter and 3 mm in length) were studied using PPMS installation. The measurements were performed in the temperature range 2–300 K with an absolute accuracy better than 1%.

Fig. 4 shows a summary of the basic magnetic characterization of CsFe$_2$F$_6$. The magnetization curves under an external magnetic field of 0.5, 5 and 20 kOe are presented in Fig. 4(a). The monotonic elevating magnetization with the magnetic field strongly increases on cooling. At about 14 K all curves $M(T)$ exhibit pronounced change in their behavior.

As shown in Fig. 4(b) the anomalous peculiarities are also characteristic for the temperature dependence of the inverse magnetic susceptibility, $1/\chi$. The $1/\chi$ value is the same at all fields studied down to temperature 13.7 ± 0.3 K (the inset of Fig. 4(b)) which is in a good agreement with temperature of the heat
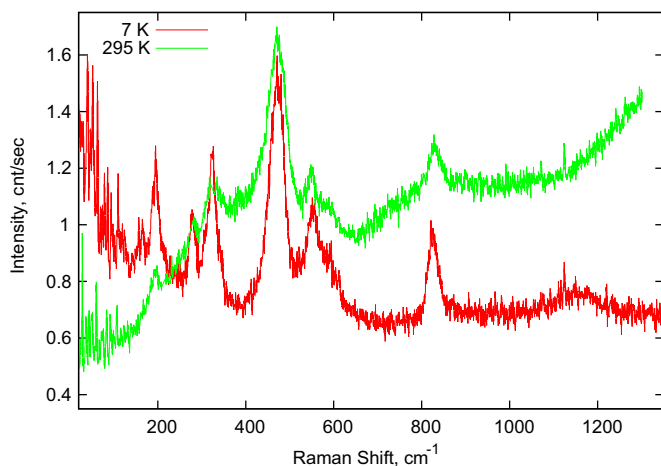

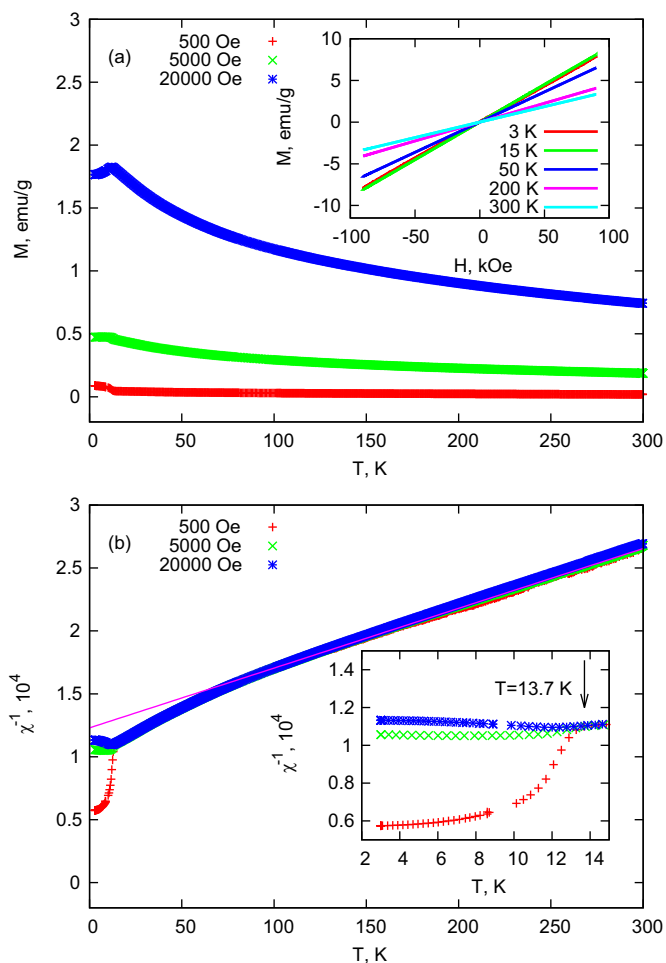**Fig. 3.** Experimental Raman spectra of the CsFe$_2$F$_6$ compound at 295 K and 7 K.

Fig. 4. Temperature dependences of (a) the d.c. magnetization, and (b) the inverse magnetic susceptibility with a Curie–Weiss fit (solid line). The inset to (a) shows the linear magnetization vs. field behavior over the whole temperature range studied. The inset to (b) shows a close up of the low temperature region.

capacity maximum (Fig. 2).

Considerable additional information can be gathered from the χ^{-1} vs. T plot shown in Fig. 4(b). The data are seen to adhere quite well to the Curie–Weiss form ($\chi = C/T - \Theta$), where C and Θ are constants for $T > 100$ K, yielding a Weiss temperature of -260 K. From temperature dependence of χ^{-1} the effective magnetic moment was defined equal to 7.7 μ_B/f.u. This value was less than theoretically found effective moment of a crystal 10.8 μ_B/f.u., which was defined from the contributions of the magnetic

moments of ions Fe^{2+} and Fe^{3+}: $S(Fe^{3+}) = 5/2$, $S(Fe^{2+}) = 2$, $g = 2$.

It is necessary to point out that measurements of $\chi(T)$ in magnetic fields in the range 500–20000 Oe yielded magnetic moment and Θ values varied by only 5%, consistent with the fact that the $M(H)$ curves are quite linear at all temperatures (inset to Fig. 4(a)). The extracted values are similarly in agreement with respect to the exact temperature range used for the fitting to the Curie–Weiss form. Importantly, the large negative Weiss temperature Θ indicates relatively strong antiferromagnetic interactions between the Fe moments. Comparison to the actual antiferromagnetic ordering temperature of 13.7 K indicates significant magnetic frustrations in this compound, with a frustration ratio (Θ/T_N) of 19 [16].

2.4. Calculations of superexchange interactions

We used simple model of indirect bond to estimate exchange interactions and magnetic structure [17–19]. The structure of $CsFe_2F_6$ contains two crystallographic nonequivalent octahedral positions of iron. According to X-ray data, the Fe1 position is located in an elongated FeF_6 octahedron, whereas Fe2 position is in a slightly compressed one. The qualitative scheme of energy levels and populations in 3d individual orbitals of Fe1 and Fe2 cations in an octahedral crystal field are presented in Fig. 5.

It is clear that Fe^{2+} cation prefers the Fe2 positions due to the structure of energy levels and a bigger volume of octahedral vacancies. Mössbauer experiment (Fig. 1) confirms the ordered distribution of Fe^{3+} and Fe^{2+} on Fe1 and Fe2 positions, respectively.

According to the model of indirect bond $CsFe_2F_6$ structure can be characterized by three parameters of cation–cation exchange interactions:

$$J_{11}(Fe^{3+} - Fe^{3+}) = -\left(b^2 + c^2\right)U_1 \cos^2\theta,$$

$$J_{12}(Fe^{3+} - Fe^{2+}) = -\left|\left(b^2 + c^2\right)(U_1 + U_2) - c^2 J^{in}\right| \cos^2\theta,$$

$$J_{22}(Fe^{2+} - Fe^{2+}) = -\left(b^2 + c^2\right)U_2 \cos^2\theta,$$

where b and c are parameters of the ligand-cation electronic transfer through σ- and π- bonds, respectively, and represent squares of admixture coefficients of the anti-connecting molecular orbitals. U_1 and U_2 are energies of electronic excitations of ligand – cation for Fe^{3+} and Fe^{2+}, respectively. J^{in} is the intra-atomic exchange energy (Hund's interaction). θ is the angle of indirect bond. The factor $\cos^2\theta$ accounts for the angle dependence of the transfer parameters.
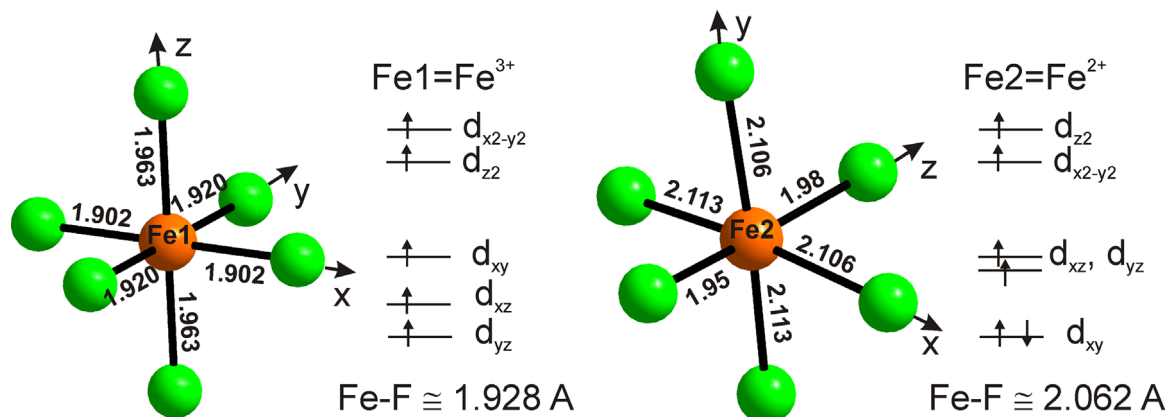

Fig. 5. The scheme of 3d-levels splitting of iron cations in $CsFe_2F_6$ structure.

Table 3
Parameters of intersublattice exchange interactions, J_{ij} (in Kelvin), and magnetic neighbors (z_{ij}) characterizing $CsFe_2F_6$ structure.

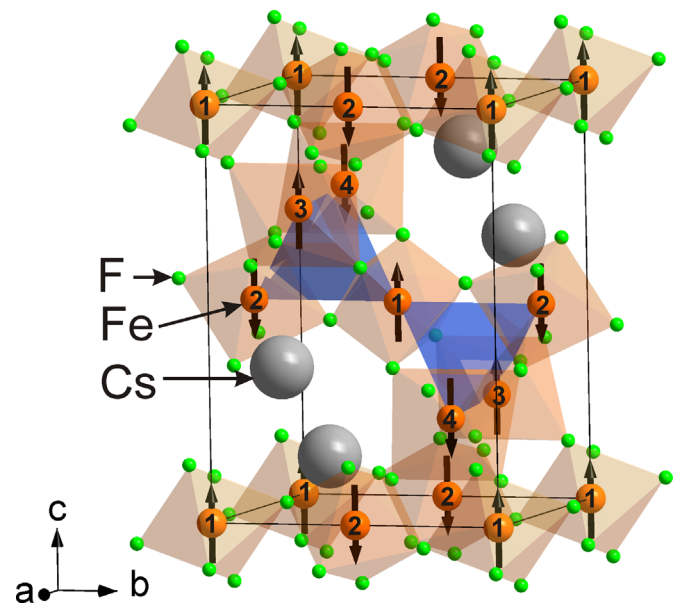|	Fe^{3+}	Fe^{2+}
Fe^{3+}	− 16.7 (2)	− 24.2 (4)
Fe^{2+}	− 24.2 (4)	− 17.3 (2)

Fig. 6. Proposed mutual orientation of the Fe ions magnetic moments in $CsFe_2F_6$ (with sublattice numbering).

Table 4
Energy of intersublattice exchange interactions, E_e (in Kelvin), characterizing $CsFe_2F_6$ structure. The strongest ordering interactions are shown in bold. The frustrating interactions are shown in italic.

	1↑	2↓	3↑	4↓
1↑	0	**− 104.4**	*− 60.5*	**− 60.5**
2↓	**− 104.4**	0	**− 60.5**	*− 60.5*
3↑	*− 60.5*	**− 60.5**	0	**− 69.1**
4↓	**− 60.5**	*− 60.5*	**− 69.1**	0

In the structure of $CsFe_2F_6$ there are two different types of (Fe^{3+}–Fe^{2+}) length bonds and angles, which can be described by identical equations. Such a difference is neglected for simplicity in the following.

Using known parameters of covalency for fluoride perovskites [17,19]: $b = 0.026$, $c = 0.012$, $U_1 = 9$ eV, $U_2 = 8$ eV, $J^{in} = 3$ eV, we can estimate the parameters of exchange interaction in two-sublattice model taking into account the number of magnetic neighbors z_{ij} (Table 3).

This set of exchange parameters leads to Neel temperature $T_N \approx 34$ K and to the paramagnetic Curie temperature $\Theta_C \approx -404$ K. When comparing with experimental $T_N = 13.7$ K and $\Theta_C = -260$ K we see that calculations overestimate these temperatures by 1.5–2 times. Such a large disagreement does not seem to be catastrophic in view that calculations in the framework of simple model of indirect bonds were performed using parameters of covalence for various fluorine compounds. The main thing is that the large difference in the values of T_N and Θ_C accounts for existence of the strong frustration effects in this type of compounds.

For an assessment of magnetic structure we break system into magnetic sublattices so that to exclude anti-ferromagnetic intra sublattice interactions. This condition is answered by four-sublattice model. Reference of cations to sublattices is shown in Fig. 6. Fe^{3+} cations form sublattices 1 and 2. Fe^{2+} cations form sublattices 3 and 4. The calculated energies of intersublattice exchange interactions $E_e = z_{ij}J_{ij}S_iS_j$ are presented in Table 4.

The arrows associated with sublattice numbers illustrate the proposed magnetic structure of the system (mutual orientation of the magnetic moments of sublattices) imposed by integrals of exchange interactions. Energies of exchanges highlighted in bold type are antiferromagnetic ordering, i.e. supporting the proposed magnetic structure. Energies, designated in the italics, are frustrating.

The proposed model of magnetic structure is in agreement with the magnetic structure of $RbFe_2F_6$ obtained from the first-principal calculations based on density functional theory using generalized gradient approximation and Hubbard U method (GGA-U) [5].

3. Conclusions

A mixed-valency metal fluoride, $CsFe^{2+}Fe^{3+}F_6$, was synthesized and characterized. The study of Mössbauer spectra has confirmed the ordered arrangement of Fe^{2+} and Fe^{3+} ions in pyrocholore-related room temperature structure. Two anomalies of heat capacity were found at 13.7 K and 30 K associated with a phase transition followed by antiferromagnetic ordering and Schottky anomaly, respectively. The study of Raman spectra revealed that orthorhombic symmetry is maintained at least down to 7 K. The total experimental magnetic entropy agrees well with the maximum magnetic entropy for Fe^{2+} and Fe^{3+} ions which were found in high-spin states according to Mössbauer data.

Magnetic measurements have shown a large negative Weiss temperature Θ indicating relatively strong antiferromagnetic interactions and significant magnetic frustrations in accordance with the high value of (Θ/T_N) = 19. In the framework of a simple model of indirect bonds, the superexchange interactions were calculated and a magnetic structure was proposed.

References

[1] A. Grzechnik, W. Morgenroth, K. Friese, Disordered pyrochlore $CsMgInF_6$ at high pressures, J. Solid State Chem. 182 (7) (2009) 1792–1797.
[2] M.S. Molokeev, E.V. Bogdanov, S.V. Misyul, A. Tressaud, I.N. Flerov, Crystal structure and phase transition mechanisms in $CsFe_2F_6$, J. Solid State Chem. 200 (0) (2013) 157–164.
[3] K.S. Aleksandrov, B.V. Beznosikov, Structural Phase Transitions in Crystals, Nauka, Novosibirsk, 1993.
[4] G. Ferey, M. Leblanc, R. De Pape, J. Pannetier, Frustrated magnetic structures: II. Antiferromagnetic structure of the ordered modified pyrochlore $NH_4Fe^{II}Fe^{III}F_6$ at 4.2 K, Solid State Commun. 53 (6) (1985) 559–563.
[5] S.W. Kim, S.-H. Kim, P.Sh Halasyamani, M.A. Green, K.P. Bhatti, C. Leighton, H. Das, C.J. Fennie, $RbFe^{2+}Fe^{3+}F_6$: synthesis, structure, and characterization of a new charge-ordered magnetically frustrated pyrochlore-related mixed-metal fluoride, Chem. Sci. 3 (2012) 741–751.
[6] E. Banks, J.A. Deluca, O. Berkooz, Preparation, magnetic properties and Mössbauer study of the modified pyrochlores, J. Solid State Chem. 6 (4) (1973) 569–573.
[7] A. Tressaud, F. Menil, R. Georges, J. Portier, P. Hagenmuller, Proprietes magnetiques des composes de type bronzes fluores M_xFeF_3 (M=K, Rb, Cs), Mat. Res. Bull. 7 (11) (1972) 1339–1346.
[8] N.P. Raju, J.E. Greedan, M.A. Subramanian, C.P. Adams, T.E. Mason, Magnetic and specific heat studies of the cation-ordered pyrochlore NH_4CoAlF_6, Phys. Rev. B 58 (1998) 5550–5553.

[9] N.N. Greenwood, F. Menil, A. Tressaud, Etude par effet Mössbauer des composes de type bronzes fluores M_xFeF_3 (M=K, Rb, Cs, NH_4), J. Solid State Chem. 5 (3) (1972) 402–409.

[10] E. Baum, P. Dahlke, V. Kaiser, M. Molinier, R.E. Schmidt, Ju Pebler, W. Massa, D. Babel, Zur kristallstruktur von pyrochloren: Mossbauer-spektrum von orthorhombischem $CsFe_2F_6$ und rontgenographische einkristall-untersuchungen an den kubischen verbindungen $CsMgGaF_6$, $CsM^{II}M^{III}F_6$ (M^{II}=Mn, Zn), $CsM^{II}Fe^{III}F_6$ (M^{II}=Mn, Cu, Zn) und Cs4Cu5V3O2F19, Z. Anorg. Allg. Chem. 632 (14) (2006) 2244–2250.

[11] K. Nakomoto, Infrared and Raman Spectra of Inorganic and Coordination Compounds, Wiley, New York, 1985.

[12] S. Milicev, A. Rahten, H. Borrmann, J. Siftar, Proton tunnelling in hydrazinium cations: Vibrational spectra of $(N_2H_5)_2HGaF_6 \cdot 2H_2O$ and $(N_2H_5)_2HFeF_6 \cdot 2H_2O$ and crystal structure of $(N_2H_5)_2HFeF_6 \cdot 2H_2O$ at various temperatures, J. Raman Spectrosc. 28 (5) (1997) 315–321.

[13] K. Weighardt, H.H. Eysel., Raman-spektren einiger hexafluorometallate (III), Z. Naturforsch. 25b (1970) 105.

[14] N.P. Raju, E. Gmelin, R.K. Kremer., Magnetic-susceptibility and specific-heat studies of spin-glass-like ordering in the pyrochlore compounds $R_2Mo_2O_7$ (R=Y, Sm, or Gd), Phys. Rev. B 46 (9) (1992) 5405–5411.

[15] J.E. Greedan, N.P. Raju, A. Maignan, C. Simon, J.S. Pedersen, A.M. Niraimathi, E. Gmelin, M.A. Subramanian, Frustrated pyrochlore oxides, $Y_2Mn_2O_7$, $Ho_2Mn_2O_7$, and $Yb_2Mn_2O_7$: bulk magnetism and magnetic microstructure, Phys. Rev. B 54 (10) (1996) 7189–7200.

[16] A.P. Ramirez, Strongly geometrically frustrated magnets, Annu. Rev. Mater. Sci. 24 (1994) 453–480.

[17] O.A. Bayukov, A.F. Savitskii., The prognostication possibility of some magnetic-properties for dielectrics on the basis of covalency parameters of ligand cation bonds, Phys. Status Solidi B 155 (1) (1989) 249–255.

[18] P.W. Anderson, New approach to the theory of superexchange interactions, Phys. Rev. 115 (1959) 2–13.

[19] M.V. Eremin., Spectroscopy of Crystals, Nauka, Leningrad, 1985.